EBioMedicine 8 (2016) 159–172

Contents lists available at ScienceDirect

EBioMedicine

journal homepage: www.ebiomedicine.com

Subcellular compartmentalization of docking protein-1 contributes to progression in colorectal cancer

Teresa Friedrich [a,1], Michaela Söhn [a,1], Tobias Gutting [a,1], Klaus-Peter Janssen [b], Hans-Michael Behrens [c], Christoph Röcken [c], Matthias P.A. Ebert [a], Elke Burgermeister [a,*]

[a] Dept. of Medicine II, Universitätsmedizin Mannheim, Medical Faculty Mannheim, Heidelberg University, Mannheim, Germany
[b] Dept. of Surgery, Klinikum rechts der Isar, Technische Universität München, Munich, Germany
[c] Institute of Pathology, Christian-Albrechts University, Kiel, Germany

ARTICLE INFO

Article history:
Received 4 January 2016
Received in revised form 19 April 2016
Accepted 4 May 2016
Available online 5 May 2016

Keywords:
Docking protein
DOK
RAS
PPAR
Colorectal cancer

ABSTRACT

Full-length (FL) docking protein-1 (DOK1) is an adapter protein which inhibits growth factor and immune response pathways in normal tissues, but is frequently lost in human cancers. Small DOK1 variants remain in cells of solid tumors and leukemias, albeit, their functions are elusive. To assess the so far unknown role of DOK1 in colorectal cancer (CRC), we generated DOK1 mutants which mimic the domain structure and subcellular distribution of DOK1 protein variants in leukemia patients. We found that cytoplasmic DOK1 activated peroxisome-proliferator-activated-receptor-gamma (PPARγ) resulting in inhibition of the *c-FOS* promoter and cell proliferation, whereas nuclear DOK1 was inactive. PPARγ-agonist increased expression of endogenous DOK1 and interaction with PPARγ. Forward translation of this cell-based signaling model predicted compartmentalization of DOK1 in patients. In a large series of CRC patients, loss of DOK1 protein was associated with poor prognosis at early tumor stages ($^{*}p = 0.001$; $n = 1492$). In tumors with cytoplasmic expression of DOK1, survival was improved, whereas nuclear localization of DOK1 correlated with poor outcome, indicating that compartmentalization of DOK1 is critical for CRC progression. Thus, DOK1 was identified as a prognostic factor for non-metastatic CRC, and, *via* its drugability by PPARγ-agonist, may constitute a potential target for future cancer treatments.

1. Introduction

Adapter and scaffold proteins rewire signaling networks by subcellular compartmentalization and enable spatio-temporal adaptation to environmental cues that may be derailed in disease conditions like cancer (Good et al., 2011). Docking protein-1 (DOK1) is a versatile adapter protein and negative regulator of signaling (Mashima et al., 2009). DOK1 belongs to a protein family which controls immune receptors in lymphocytes and myeloid cells and inhibits inflammation *in vivo* (Shinohara et al., 2005). *Dok1*-deficient mice suffer from hematopoietic defects (Yasuda et al., 2004) and, together with loss of other DOK members, succumb to aggressive sarcomas (Mashima et al., 2010). DOK1 inhibits cytosolic (CTK) or receptor (RTK) tyrosine kinases and binds p120 RAS GTPase-activating protein (GAP) to dampen proliferation *via* the

Abbreviations: a-C, anti-C-terminal; a-N, anti-N-terminal; Ab, antibody; ACO, acyl CoA oxidase; AF, activating function; BCCL, B-cell chronic lymphocytic leukemia; CAV1, caveolin-1; CCLE, cancer cell line encyclopedia; CDK, cyclin-dependent protein kinase; CK, casein kinase; CoIP, coimmunoprecipitation; CRC, colorectal cancer; CTK, cytosolic tyrosine kinase; CYT, cytoplasm; DBD, DNA-binding domain; DC, C-terminal (p44) cytoplasmic truncation mutant of FL p62 DOK1; DN, N-terminal (p33) nuclear truncation mutant of FL p62 DOK1; DOK1, docking protein-1; EGF, epidermal growth factor; ER, endoplasmic reticulum; ERK, extracellular signal-regulated protein kinase; EV, empty vector; FFPE, formalin-fixed paraffin-embedded; FL, full-length; FOS, FBJ murine osteosarcoma viral oncogene homolog human; G, tumor grade; GAP, GTPase activating protein; GC, gastric cancer; H7, helix-7; HE, hematoxylin eosin; HRP, horse radish peroxidase; HYB, Hakai-like PY-binding domain; IB, immunoblot; IHC, immunohistochemistry; INS, insoluble; IP, immunoprecipitation; LBD, ligand-binding domain; M, distant metastasis; MAPK, mitogen-activated protein kinase; MEK, MAPK kinase; MTT, 3-(4,5-dimethylthiazol-2-yl)-2.5-diphenyltetrazolium bromide; N, nodal spread; NC, normal colon tissue; NES, nuclear export signal; NLS, nuclear localization signal; NR, no relapse; NUC, nucleoplasm; OD, optical density; OS, overall survival; PH, plextrin homology; PLA, proximity ligation assay; PPARγ, peroxisome proliferator-activated receptor gamma; PPRE, PPARγ-responsive element; PTB, phospho-tyrosine binding; pTNM, tumor classification system; PY, phospho-tyrosine; R, relapse; RA, point mutant of the PTB domain; RAS, rat sarcoma viral oncogene homolog human, rosi rosiglitazone; RTK, receptor tyrosine kinase; RXR, retinoid X receptor; SI, small intestine; SRC, Rous sarcoma proto-oncogene; SRE, serum response element; T, local tumor growth; TCL, total cell lysate; TFF, trefoil factor; TMA, tissue microarray; TSS, tumor-specific survival; TU, colon tumor tissue; UICC, union internationale contre le cancer; UPL, universal probe library; WT, wild-type.

* Corresponding author at: Department of Medicine II, Universitätsmedizin Mannheim, Medical Faculty Mannheim, Heidelberg University, Theodor-Kutzer Ufer 1-3, D-68167 Mannheim, Germany.
E-mail address: elke.burgermeister@medma.uni-heidelberg.de (E. Burgermeister).
[1] Equal author contribution.

http://dx.doi.org/10.1016/j.ebiom.2016.05.003

extracellular signal-regulated protein kinase-1/2 (ERK1/2) and other signaling cascades in non-hematopoietic cells (Songyang et al., 2001; Shinohara et al., 2004; Zhao et al., 2006). DOK1 sensitizes human cancer cells to apoptosis by etoposide, emphasizing its role in tumor suppression (Siouda et al., 2012).

Alternative translation initiation yields several protein isoforms encoded by the same *DOK1* mRNA (Kobayashi et al., 2009). Full-length (FL) p62 DOK1 has an N-terminal plextrin homology (PH) domain for membrane binding, a phospho-tyrosine-binding (PTB) domain for interaction with phospho-tyrosine substrates (*e.g.* growth factor receptors, integrins, *etc.* (Oxley et al., 2008)) and a C-terminal domain with proline and phospho-tyrosine residues which bind SH3-domains and SRC kinase, respectively. The C-terminal part of DOK1 also interacts with p120RASGAP, SH2 (Songyang et al., 2001; Shinohara et al., 2004) and other PTB domains (*e.g.* hakai (Mukherjee et al., 2012)) and contains a nuclear export signal (NES) (Niu et al., 2006) that mediates nucleo-cytoplasmic shuttling of DOK1. FL p62 DOK1 localizes to the nucleus in starved or suspended cells, to the plasma membrane and the cytosol in growth factor-stimulated and adherent cells, consistent with tyrosine kinase inhibition at membranes (Niu et al., 2006). N-terminally truncated DOK1 (p37–44) lacks the PH-domain, locates to the perinuclear area and may be responsible for transport between cytosol and nucleus (Kobayashi et al., 2009). Small DOK1 (p19–22) is deficient of both the PTB and the C-terminal domains (Hubert et al., 2000). Polymorphisms and frame shift mutations in human leukemias (Lee et al., 2004; Lee et al., 2007) introduce aberrant stop codons that yield C-terminally deleted DOK1 (p33–35) isoforms with a nuclear localisation signal (NLS) which are confined to the nucleus as well. Splice variants or dominant-negative mutants were also described for other DOK family members (Hosooka et al., 2001; Baldwin et al., 2007; Hamuro et al., 2008). However, the function of subcellular compartmentalization of DOK mutants remains unknown.

Loss of FL p62 DOK1 as a tumor suppressor is a common event in human cancers, including solid tumors (Berger et al., 2010; Saulnier et al., 2012). Oncogenic kinases (Janas and Van Aelst, 2011; Miah et al., 2014) and viruses (Siouda et al., 2014) facilitate proteasomal degradation of DOK1 and epigenetic silencing of the *DOK1* gene. In contrast, agents that promote stress responses (such as E2F) (Siouda et al., 2012) and differentiation, *e.g.* ligands for peroxisome proliferator-activated receptor-gamma (PPARγ) (Hosooka et al., 2008; Burgermeister et al., 2011), up-regulate DOK1 expression. DOK1 counteracts inactivation of PPARγ by the RAS-ERK1/2 pathway in human cells (Demers et al., 2009; Burgermeister et al., 2011) and mice (Hosooka et al., 2008; Jiang et al., 2015).

DOK1 also triggers apoptosis by recruiting and interacting with SMADs (Yamakawa et al., 2002) and inhibits expression of inflammatory genes driven by NFκB and STATs (Nold-Petry et al., 2015) in hematopoietic cells. Genomic alterations of *SMAD3*, *P53*, *RAS*, and *APC* are hallmarks of colorectal cancer (CRC) (Kodach et al., 2008). We therefore hypothesized that transcription factors are down-stream effectors of DOK1 mutants in human cancer cells, where FL p62 DOK1 is lost.

We demonstrate here that DOK1 activated the ligand-dependent transcriptional activity of PPARγ and inhibited activation of the human *c-FOS* promoter downstream of RAS, resulting in reduced cell proliferation. This anti-tumor mechanism was allocated to protein domains and subcellular compartmentalization of DOK1 protein variants. Collectively, our patient data propose DOK1 as a prognostic factor and potential drugable target for human CRC.

2. Materials and methods

2.1. Patients

Tissue specimens of primary CRC cases were obtained from 1648 patients who had undergone elective surgery for CRC at the University Hospital Kiel (1995–2009). Inclusion criteria and clinico-pathological characteristics of the study population are summarized in (Ingold Heppner et al., 2014). For histology, formalin-fixed [in 10% neutralized formalin] and paraffin-embedded (FFPE) tissue samples were stained using hematoxylin and eosin (HE). Tumors were classified according to the WHO classification, and the pTNM stage was determined according to the seventh edition of the UICC guidelines. FFPE tissue samples were used to generate custom-made tissue microarrays (TMAs) as described (Kononen et al., 1998). Fresh-frozen patient tissue specimens from the University Hospital Munich comprising matched CRC tumor (TU), adjacent normal colon (NC) and liver metastases (M) were graded by histopathological evaluation (stages II–IV) on HE-stained cryosections. Mutations of *KRASG12*, *KRASG13* and *BRAFV600E* were evaluated by high resolution melting (Ebert et al., 2012). The study was approved by the Ethics Committees of the Universities of Kiel, Heidelberg and Munich, Germany. Commercial TMAs (Co483) were purchased from US Biomax, Rockville, MD, USA.

2.2. Animals

Studies on wild-type (WT) (C57BL6J, Charles River, Wilmington, MA) were approved (Az35-9185.82-G-176-12) by the government of Baden-Württemberg, Karlsruhe, Germany.

2.3. Reagents

Chemicals were from Merck (Darmstadt) or Sigma (Steinheim, Germany), rosiglitazone (rosi, #71740) from Cayman (Ann Arbor, MI). Abs were GFP (#11814460001, Roche, Mannheim, Germany), FLAG (F7425, Sigma), DOK1 (M-19, sc-6277; A3, sc-6929), PPARγ (sc-7273; sc-7196), CAV1 (sc-894), HSP90 (sc-7947), lamin AC (sc-20681) (all from Santa Cruz Biotech., CA), phospho-S82(84) PPARγ (AW504, Upstate Millipore, Schwalbach, Germany), DOK1 (ab8112), POM121 (ab190015, both from Abcam, Cambridge, UK), calnexin (#2433), PPARγ (#2435), ERK1/2 (#4370) (all from Cell Signaling, Danvers, MA), pan-RAS (#R1198-01D, US Biological, Biomol, Hamburg, Germany), villin (#3722, Epitomics, Burlingame, CA). *DOK1* siRNA and control were from Dharmacon (Thermofisher Scientific, Waltham, MA).

2.4. DNA-constructs

Serum-response element (SRE) plasmid was from Stratagene (Agilent, Santa Clara, CA). 3xPPRE-pTK-luc, GFP-PPARγ and PPARγ1-mutant H7 with deletion in helix 7 of the ligand-binding domain (LBD) were mentioned before (Burgermeister et al., 2011). PPARγ1-mutant Dbox (Zechel et al., 1994) was generated by deletion of 149DLNCRIHKKSRN160 in the DNA-binding domain (DBD), point mutant S84A by replacement of serine with alanine in the MAPK motif 83A**S**PPYYSEKT92 in the AF1 of PPARγ1 (P37231-2) (Diradourian et al., 2005). Human FL DOK1 (start codon MDGAV, aa 1–481, 62 kDa, NM_001381.3) (Songyang et al., 2001), N-terminal truncation mutant DN (start codon MDGAV, aa 1–280, 33 kDa) (Lee et al., 2004; Lee et al., 2007) and C-terminal truncation mutant DC (start codon MLENS, aa 140–481, 44 kDa) (Kobayashi et al., 2009) were amplified by PCR from cDNA of SW480 cells and inserted with or without N-terminal FLAG-tag into pTarget (Promega GmbH, Mannheim, Germany). FL and DC point DOK1 (Q99704) mutants NES (348**LL**KAK**L**353 to 348AAKAKA353) and RA (R207A, R208A, R222A, R223A) were generated as detailed by the manufacturer (Quickchange, Stratagene).

2.5. Cell culture and assays

Human embryonic kidney (HEK293T), colorectal (CRC) (SW480, HCT116, HT29, Caco2) and gastric (GC) (AGS, MKN45) cancer cell lines (American Type Culture Collection, Rockville, MD) were maintained as recommended by the distributor. Transfection and luciferase assays were described elsewhere (Burgermeister et al., 2007). The 3-

(4,5-dimethylthiazol-2-yl)-2,5-diphenyltetrazolium bromide (MTT) proliferation assay was conducted according to the manufacturer (Roche Diagnostics).

2.6. Cell fractionation, coimmunoprecipitation (CoIP), GST-pulldown, Western blot

The methods were performed as described (Burgermeister et al., 2007). Kits for RAS GTPase pulldown assays were from Biocat (Heidelberg, Germany).

2.7. Immunofluorescence microscopy

Staining and image acquisition was done as before (Burgermeister et al., 2011). Proximity ligation assay (PLA) was performed as described by the manufacturer (Duolink, Olink Bioscience, Uppsala, Sweden). Automatic counting of fluorescence signals (n > 50 per field , $n = 5$ fields per image) from Abs and DAPI was conducted with Image J (imagej.nih.gov/ij).

2.8. Immunohistochemistry (IHC)

Ab and HE stainings were done as published (Ebert et al., 2012). In brief, antigen retrieval was performed by heating of deparaffinized sections in citrate buffer (10 mM citric acid pH 6.0, 0.05% (v/v) Tween 20, H-3300) and incubated with H_2O_2 Block and Ultra V Block (both Thermo Scientific, Braunschweig, Germany) to avoid unspecific reactions. Rabbit polyclonal DOK1 (ab8112) Ab was diluted 1:800. For visualization, the ImmPRESS-HRP-Universal-Antibody Polymer and the NovaRED substrate kit (both from VectorLabs, Peterborough, UK) were applied. Mouse monoclonal DOK1 (A3) Ab was diluted 1:200, and staining was processed according to the protocol from Vectastain ABC (HRP) kit (Vectorlabs). For detection, the substrate 3,3′-diamino benzidine (brown color) was used (Vectorlabs). Counterstaining was done with hematoxylin (Dr. K. Hollborn & Söhne GmbH & Co KG; Leipzig, Germany). The frequency and intensity of DOK1 positivity was analysed in custom-made ($n = 1648$ CRC patients, from CR, Kiel (Ingold Heppner et al., 2014)) and commercial ($n = 40$ CRC patients, $n = 8$ normal human colon, CO483, US Biomax) TMAs (Boger et al., 2015; Metzger et al., 2016). The staining scores were defined as follows: 0+ = negative (0–25%), 1+ = weak (25–50%), 2+ = moderate (50–75%), 3+ = strong (75–100% positive rate compared to total cell number per field). In tumor and stroma cells, nuclear, perinuclear and cytoplasmic stainings were evaluated. Signals from Abs were quantified manually and rater-blinded at a standard bright-field microscope using Image J (imagej.nih.gov/ij) (n > 50 per field ; $n = 5$ fields per image).

2.9. Reverse transcription PCR (RT-PCR) and quantitative PCR (qPCR)

Assays were performed as published (Ebert et al., 2012). Primers and probes for RT-qPCR from the Universal Probe Library (UPL) system (Roche Diagnostics) are listed in Table S1.

2.10. Software tools and statistics

The statistical evaluation of IHC data from patients' TMAs was performed using SPSS version 20.0 (IBM Corporation, Armonk, NY) as detailed in (Boger et al., 2015; Metzger et al., 2016). The cut-off values for dichotome analysis of staining scores (0 to 3+) were calculated as ≥2.0 for tumor and ≥0.6 for stroma positivity. Univariate and multivariate analyses followed by logistic Cox regression were conducted to identify significant differences between patient groups using log-rank and Fisher exact tests. Data from *in vitro* studies are means ± S.E. from at least 3 independent experiments from different cell passages or individuals (frozen samples from mice or patients). Optical densities (OD) of bands in gels from Western blots (Fusion Solo, VWR, Radnor, Pennsylvania) and PCRs (GelIX Imager, INTAS, Göttingen, Germany) were collected using automated imaging devices and quantified with Image J (imagej.nih.gov/ij). Data were normalized to house keeping genes (*B2M*, *B2m*) or proteins (HSP90, lamin AC, β-actin) and calculated as -fold or % compared to control. Statistical analysis was done with Graphpad Prism (version 4.0, La Jolla, CA). All tests were unpaired and two-sided if not stated otherwise. *P*-values < 0.05 were considered significant (*). Signaling pathways were depicted with CellDesigner (version 4.2, systems-biology.org). Bioinformatic data were retrieved from cbioportal.org according to the TCGA publication guidelines (Cerami et al., 2012; Gao et al., 2013).

3. Results

3.1. Expression of DOK1 protein variants in cells and tissues

For validation of DOK1 antibodies, we selected four human CRC (SW480, HCT116, HT29, Caco2) and one non-cancer (HEK293T) cell line which differ in their *KRAS* and *BRAF* mutation status (Jhawer et al., 2008). Consistent with previous results in seven human gastric cancer (GC) (Burgermeister et al., 2011) and pancreatic cancer (PANC1) cells (Kobayashi et al., 2009), Western blots (Fig. 1A) of total cell lysates (TCLs) using an Ab against the N-terminal (A3) half of the protein (covering the PH and PTB domains) (Shinohara et al., 2004; Hosooka et al., 2008) detected a predominant DOK1 protein of 37 kDa.

Abs which recognized the C-terminus (M19 (van Dijk et al., 2000), ab8112 (Siouda et al., 2014)) of FL p62 DOK1 revealed a band of 44 kDa size. FL p62 DOK1 and the 19–22 kDa variants (Hubert et al., 2000) were not found in any of the cell lines. In contrast, FL p62 DOK1 was present together with smaller isoforms in whole tissue lysates from tumor (TU) and matched normal colon (NC) samples of CRC patients and intestinal organs of C57BL6J mice (Fig. 1B). Thus, DOK1 protein variants could be distinguished by domain-selective Abs (Fig. 1C) in CRC cells and tissues similar to human leukemias (Lee et al., 2004, 2007).

3.2. N- and C-terminal domains determine subcellular localization of DOK1

We then elucidated whether DOK1 variants are subjected to subcellular compartmentalization in human CRC cells as observed in leukemias. To this end, immunofluorescence microscopy was performed in SW480 and HCT116 cells (Fig. 2A). Anti-N Ab visualized a constitutive DOK1 signal in the nucleus, anti-C Ab a steady-state cytoplasmatic and perinuclear distribution of DOK1. Rapid translocations upon stimulation (such as serum or EGF e.a.) were not observed (not shown). Subcellular fractionation (Fig. 2B) confirmed that anti-N Ab detected p37 DOK1 enriched in the nucleus (NUC) (by 3 to 6-fold) compared with the cytoplasm (CYT) and the insoluble (INS) fraction in HEK293T and CRC cell lines (SW480, HCT116, HT29, Caco2). There was no colocalization between nuclear pore components (POM121) and DOK1 detected by either Ab. Instead, a partial overlap between calnexin, a marker for the endoplasmic reticulum (ER), and perinuclear DOK1 staining was observed (Fig. 2C) (Niu et al., 2006; Kobayashi et al., 2009). In frozen samples from mouse and human NC tissues, anti-C Ab again recognized cytosolic and insoluble p44 and p62 DOK1 but only low levels in the nucleus (Fig. 2D). Thus, C-terminal epitopes were correlated with cytoplasmic, N-terminal ones with nuclear distribution of DOK1 variants. The distribution was different in normal *vs.* malignant cells, evident in loss of insoluble and cytoplasmic *vs.* gain of nuclear DOK1.

To mimic the modular structure of the endogenous DOK1 variants and to understand their functional domains, we generated expression plasmids for p33 DN (**PH**$^+$, **PTB**$^+$, NES$^-$) (Lee et al., 2004, 2007) and

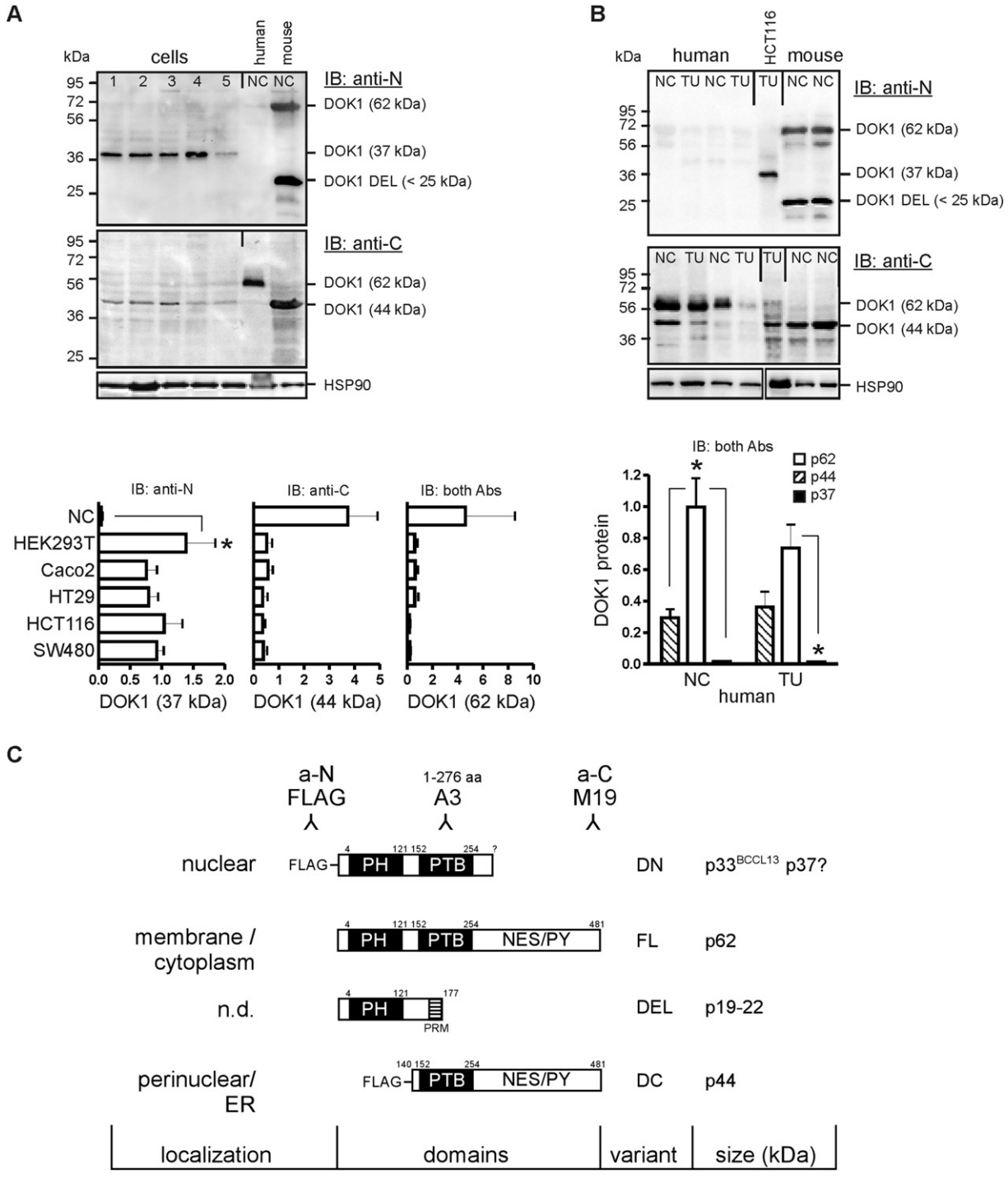

Fig. 1. Expression of DOK1 protein in CRC cells and tissues. (A) Top: Detection of DOK1 variants in human transformed and CRC cell lines (1 = SW480, 2 = HCT116, 3 = HT29, 4 = HEK293T, 5 = Caco2) using domain-specific antibodies (Abs). Total cell lysates (TCLs) were subjected to Western blotting with anti-N (A3) or anti-C (M19) DOK1 Abs. Bottom: O.D. values of bands in gels were normalized to HSP90 and calculated as -fold ± S.E. *vs.* normal colon (NC) tissue ($n = 3$ per cell line, $^*p < 0.05$ *vs.* NC, Kruskal Wallis test). NC control is the mean of $n = 5$ healthy individuals. (B) DOK1 variants in intestinal tissues. Top: Whole tissue lysates from frozen samples of matched tumor (TU) and normal colon (NC) specimens from CRC patients (or C57BL6J mice as control) were analysed as in A. Bottom: Quantitative data are -fold ± S.E. ($n = 15$ cases, $^*p < 0.05$ *vs.* p62, two-way ANOVA). (C) Scheme of human DOK1 protein variants. Legend: FL = full-length p62 DOK1, DC = p44 C-terminal part of DOK1 (Kobayashi et al., 2009), DN = p33–37 N-terminal part of DOK1, DEL = small p19–22 deletion variant of DOK1 (Hubert et al., 2000), C = C-terminus, N = N-terminus, BCCL13 = leukemia variant (Lee et al., 2004, 2007). Subcellular localization and Ab binding epitopes are depicted.

p44 DC (PH^-, **PTB^+**, **NES^+**) (Kobayashi et al., 2009) (see model in Fig.1C). Immunofluorescence stainings with FLAG-Ab visualized both DOK1 truncation mutants upon transfection into HEK293T cells (Fig. 3A). Due to absence of the NES (Lee et al., 2004, 2007), DN was enriched in the nucleus, whereas DC, because of its functional NES (Kobayashi et al., 2009), remained in the cytosol. Anti-C Ab detected FL p62 DOK1 and DC but not DN, while anti-N Ab (FLAG) recognized both mutants (Fig. 3B). Subcellular fractionation confirmed that the N-terminal part of DOK1 goes to the nucleus, whereas the C-terminal half stays in the cytoplasm.

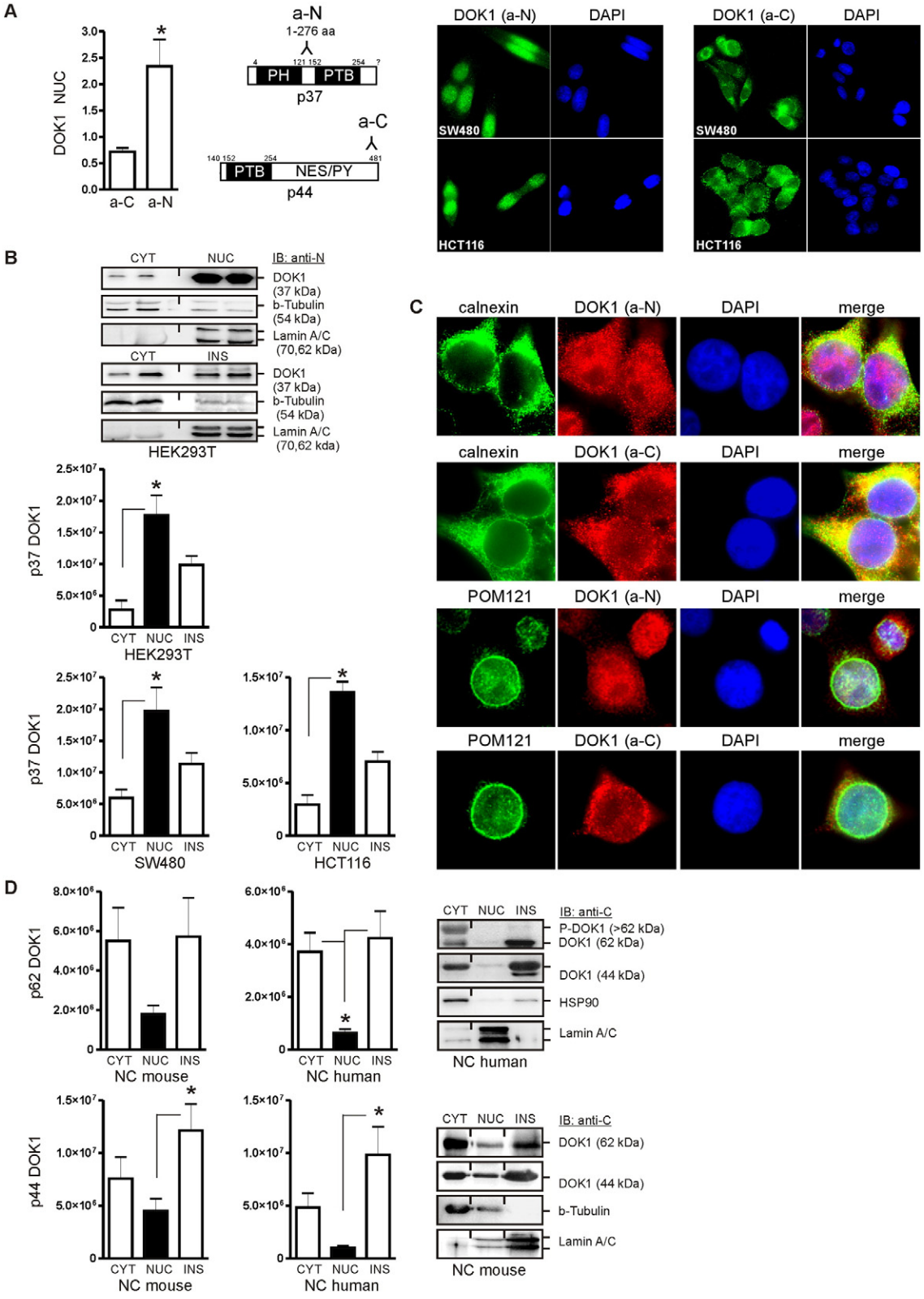

Fig. 2. Subcellular localization of DOK1 protein variants. (A) Anti-N Ab (a-N) recognizes nuclear DOK1, anti-C Ab (a-C) cytoplasmic DOK1. Cycling cells were fixed and stained for immunofluorescence microscopy. Data show enrichment of DOK1 signals detected by a-N Ab in the nucleus (NUC) as -fold ± S.E. compared to a-C Ab ($n = 3$ per cell line, > 30 nuclei per field, $n = 5$ fields, $^*p < 0.05$ a-N *vs.* a-C; Mann Whitney test). Colors: green = DOK1, blue = nuclei; Magnification 630×. (B) Anti-N Ab detects p37 DOK1 in the nucleus of malignant cells. Cells were subjected to subcellular fractionation and Western blotting. O.D. values from bands in gels are means ± S.E. of DOK1 protein per fraction ($n = 3$ per cell line, $^*p < 0.05$ *vs.* NUC; Kruskal Wallis test). Legend: CYT = cytoplasm, NUC = nucleus, INS = insoluble membrane and matrix fraction (cytoskeleton, chromatin e.a.). (C) Anti-C Ab detects colocalization of cytoplasmic DOK1 with calnexin (ER marker) but not with POM121 (ENV marker) in the perinuclear area of the endoplasmic reticulum (ER) and the nuclear envelope (ENV). Anti-N Ab detects overlay of nuclear DOK1 with nuclei (DAPI). HEK293T cells were analysed as in A. Colors: green = organelle marker, red = DOK1, blue = nuclei; Magnification 630×. (D) Anti-C Ab detects FL p62 and p44 DOK1 in the cytoplasm and insoluble fraction of non-malignant cells. Fresh-frozen normal colon (NC) tissue from patients or C57BL6J mice was subjected to fractionation as in B. Results are shown as in B ($n = 3$ per species, $^*p < 0.05$ *vs.* NUC, Kruskal Wallis test).

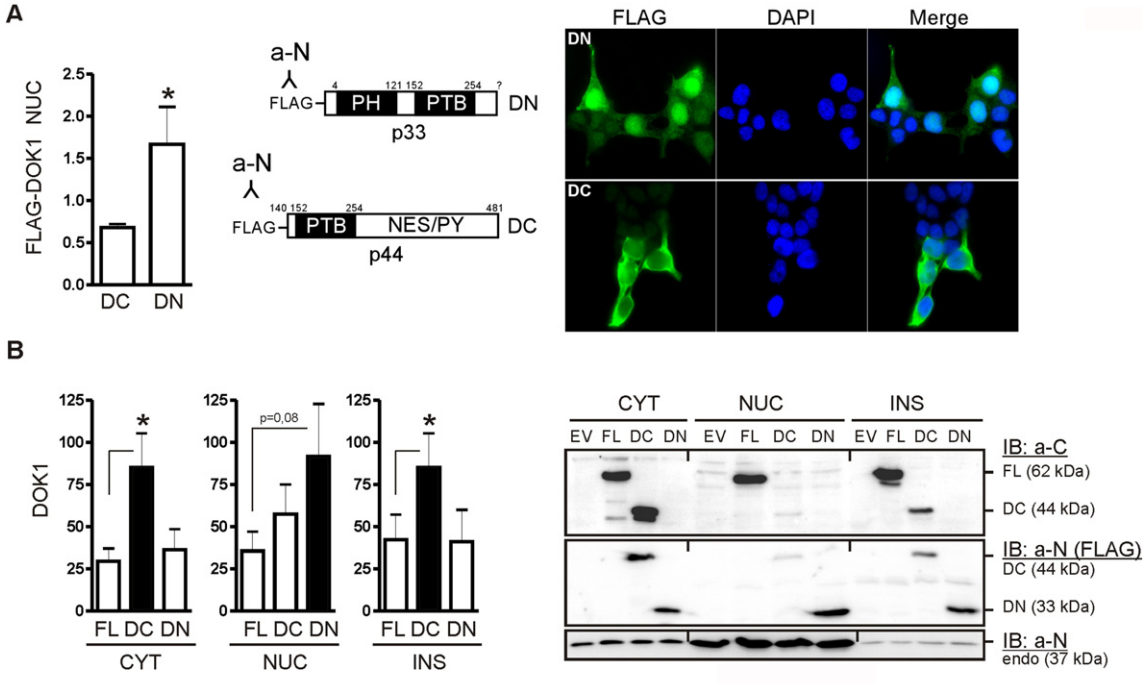

Fig. 3. N- and C-terminal domains determine subcellular localizations of DOK1. (A) Ectopic DOK1 mutants mimic compartmentalization of endogenous DOK1 protein variants. HEK293T cells were transfected with expression plasmids encoding FL p62 DOK1 or the FLAG-tagged truncation mutants p33 DN and p44 DC for 48 h before immunofluorescence staining using FLAG Ab. Colors: green = FLAG-DOK1, blue = nuclei; Magnification 630×. Data show enrichment of DN in the nucleus (NUC) as -fold ± S.E. compared to DC ($n = 3$ per mutant, > 50 nuclei per field, $n = 5$ fields, *$p < 0.05$ DN *vs.* DC, Mann Whitney test). (B) DN is targeted to the nucleus, DC to the cytoplasm. HEK293T cells were transfected as in A. TCLs were subjected to subcellular fractionation and Western blotting using anti-N (FLAG) and anti-C DOK1 Abs. O.D. values normalized to HSP90 or lamin AC are -fold ± S.E. of DOK1 protein per fraction ($n = 3$, *$p < 0.05$ mutant *vs.* FL, Kruskal Wallis test).

3.3. DOK1 mutants alter the subcellular localization of PPARγ

As an exemplary target of DOK1, we studied the localization and activity of PPARγ, a transcription factor downstream of and inhibited by the RAS-ERK1/2 cascade (Burgermeister et al., 2007; Banks et al., 2015). HEK293T cells were transfected with DOK1 truncation mutants for 48 h followed by immunofluorescence staining with PPARγ Ab (#2435). In cycling cells transfected with empty vector (EV), endogenous PPARγ signals were mainly cytosolic in the perinuclear area. DN (NES^-) evoked an enrichment of PPARγ in the nucleus (by 2 to 3 -fold *vs.* EV), and subcellular fractionation confirmed this observation (**S1**). FL (NES^+) and DC (NES^+) had no effect on PPARγ distribution (not shown). Thus, N-terminal domains confer nuclear, C-terminal domains cytoplasmatic localization of PPARγ. To identify peptide motifs responsible for DOK1 and PPARγ distributions, two additional point mutants were generated in FL p62 DOK1. The nuclear export signal (NES3 according to (Niu et al., 2006)) was deleted ("NES") and arginines R207–R208 and R222–R223, essential for interaction of the PTB domain with phospho-tyrosine substrates (Oxley et al., 2008), were mutated to alanine ("RA"). NES (NES^-) evoked an accumulation of PPARγ in the nucleus (by 2 to 3-fold *vs.* EV) (**S1**), whereas FL (NES^+) and RA (NES^+) had no effect (not shown). Hence, only NES-deficient (NES^-) DOK1 mutants forced PPARγ into the nucleus. Similar results were obtained for HCT116 and SW480 cells (not shown). Thus, the PTB core and the NES harbour amino acid residues important for spatial control of PPARγ.

3.4. DOK1 forms a complex with PPARγ

To decide whether the effect of DOK1 mutants on the localization of PPARγ is mediated by interaction, coimmunoprecipitation (CoIP) of whole tissue lysates from frozen samples of CRC patients was performed (Fig. 4A). Immunoprecipitation ("IP") was done with PPARγ Ab (H-100) and immunoblot ("IB") with anti-C DOK1 Ab. Endogenous FL p62 DOK1 was coprecipitated both in TU and NC samples. The interaction was stronger (2.5-fold NC *vs.* TU) in non-malignant tissue than in CRC, consistent with loss of FL p62 DOK1 in transformed cells. To visualize binding complexes, HEK293T cells were incubated for 16 h with vehicle (DMSO) or the PPARγ-agonist rosiglitazone (rosi, 10 μM), and proximity ligation assay (PLA) was performed using anti-N DOK1 and PPARγ (#2435) Abs (Fig. 4B). Colocalization was increased in the cytoplasm upon ligand treatment (by 7-fold *vs.* DMSO) and appeared as pink dots. No colocalization was seen in control stainings using only one Ab in the PLA reaction. Thus, there is a constitutive interaction of endogenous DOK1 with PPARγ which can be enhanced by PPARγ-agonist. Interactions between small DOK1 variants and PPARγ in human cancer cell lines (AGS, MKN45, SW480, HCT116, HT29) were weak (not shown), indicative of a loss of complex formation upon transformation.

To map the interaction sites on DOK1 and PPARγ, binding of mutant proteins was quantified in CoIPs. HEK293T cells were transfected with FLAG-DN or -DC together with GFP-PPARγ. IP was performed with GFP Ab and IB with FLAG Ab and *vice versa* (**S2**). DC and DN were both sufficient for interaction with PPARγ. To identify counterpart binding sites on both proteins, two *bona fide* docking motifs in PPARγ were tested as candidates, the S84A point mutant, which prevents phosphorylation of the receptor by MAPKs (Adams et al., 1997), and the Dbox deletion mutant that abrogates heterodimerization with RXR and DNA-binding of PPARγ (Zechel et al., 1994). The GFP-PPARγ-S84A and -Dbox mutants were cotransfected with DC-WT, -RA and -NES plasmids. S84A bound stronger to DOK1 than WT. However, dual combinations of mutants, such as S84 and DC-RA or Dbox and DC-NES, fully abolished the interaction. Thus, the tested pairs of peptide motifs (PTB^{DOK1}-$S84^{PPARγ}$; NES^{DOK1}-$Dbox^{PPARγ}$) contribute to the interaction of the two proteins (see model in **S2**).

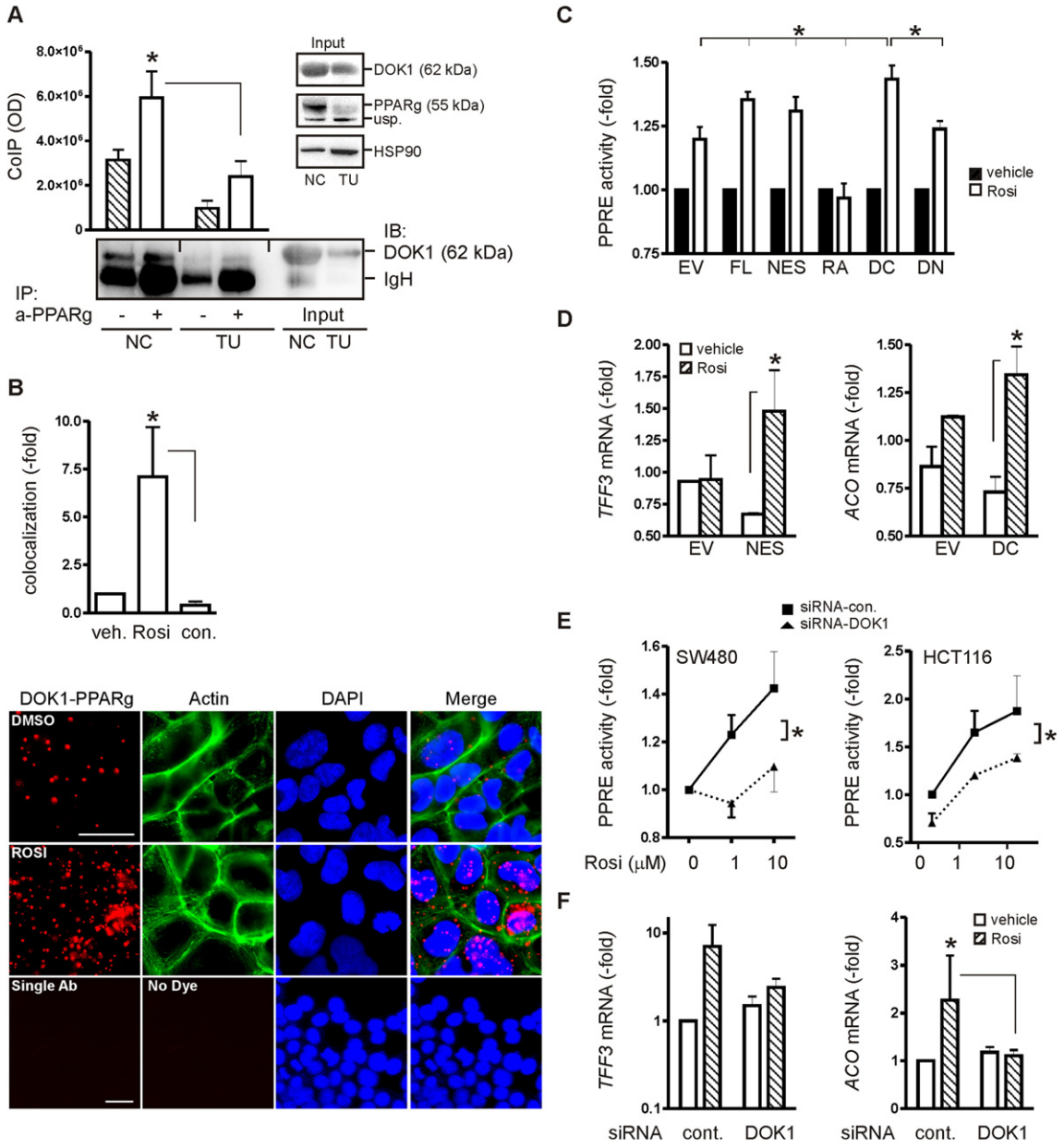

Fig. 4. DOK1 forms a complex with and increases transcriptional activity of PPARγ. (A) CoIP of FL p62 DOK1 and PPARγ from whole tissue lysates of matched frozen human TU and NC specimens. Proteins were immunoprecipitated ("IP") with PPARγ (H100) or no Ab (bead control). Coprecipitated proteins were detected ("IB") with anti-N DOK1 Ab. Results are means ± S.E. ($n = 3$ patients, *p < 0.05 NC *vs.* TU, two-way ANOVA). (B) Proximity ligation assay (PLA). HEK293T cells were serum-deprived for 16 h followed by incubation with rosi (at 10 μM) or vehicle (DMSO) for 24 h. Immunofluorescence stainings were done with anti-N DOK1 and PPARγ (#2435) Abs or single Ab (negative control). Results are -fold ± S.E. ($n = 3$ per treatment, > 50 nuclei per field, $n = 5$ fields, *$p < 0.05$ *vs.* rosi, Kruskal Wallis test). Colors: pink dots = DOK1–PPARγ colocalization, green = actin (phalloidin or "no dye" negative control), blue = nuclei; Magnification 630× and 400×. (C) DOK1 promotes transcriptional activity of PPARγ. HCT116 cells were cotransfected with DOK1 and PPRE reporter plasmids for 24 h followed by treatment with 1 μM rosi for 24 h. Luciferase activity in TCLs normalized to protein content was calculated as -fold ± S.E. ($n = 3$, *p < 0.05 DOK1 + rosi *vs.* EV + rosi, Kruskal Wallis test). PTB and C-terminal domains, but not the N-terminal part of DOK1, are required for PPARγ activation. (D) DOK1 increases PPARγ-target gene expression. Cells were transfected and treated as above. Normalized CT-values from RT-qPCRs are -fold ± S.E. ($n = 3$, *p < 0.05 rosi *vs.* vehicle, Friedmann test). (E) DOK1 knock-down decreases PPARγ-activity. Cells were cotransfected with PPRE reporter plasmid and siRNA (at 100 nM) for 24 h and treated with 1 μM rosi for additional 24 h. Data are shown as in C ($n = 3$ per cell line, *p < 0.05 DOK1- *vs.* control-siRNA; two-way ANOVA). (F) DOK1 knock-down reduces PPARγ-target gene expression. Cells were treated as in E and data are presented as in D ($n = 3$, *p < 0.05 DOK1- *vs.* control-siRNA, Friedmann test).

3.5. DOK1 promotes the transcriptional activity of PPARγ

To determine if DOK1 also alters the activity of PPARγ, HCT116 cells were transfected with DOK1 and a PPARγ-responsive (PPRE) reporter plasmid followed by a 48 h treatment with rosi (1 μM) (Fig. 4C). Luciferase activity assays showed that FL p62 DOK1 and NES increased ligand-dependent transcription (to 150 and 130% *vs.* EV). RA was unresponsive, consistent with the observation that an intact PTB domain was required for interaction with and activation of PPARγ. DC stimulated transcription (to 140%), whereas DN was inert. Similar results were obtained from HEK293T cells, whereas SW480 cells were resistant, presumably due to strong RAS activity caused by mutated *KRASG12V* alleles that lead to cytosolic retention and inactivation of PPARγ by MEK1 and ERK1/2 (Diradourian et al., 2005; Burgermeister et al., 2007).

RT-qPCRs measuring mRNA levels of trefoil factor-3 (*TFF3*) and acyl-CoA oxidase (*ACO*) confirmed up-regulation of PPARγ-target genes by DOK1 (Fig. 4D). Again, the C-terminal part of DOK1 with a functional PTB was required for ligand-dependent activation of PPARγ. In line with previous results from HEK293T and MKN45 cells (Burgermeister et al., 2011), transient knock-down of endogenous DOK1 by siRNA in HCT116 and SW480 cells decreased ligand-dependent PPARγ activation (by 20 to 50% *vs.* control-siRNA) (Fig. 4E). Reduction of *TFF3* and *ACO* mRNA levels upon DOK1 knock-down (Fig. 4F) further corroborated the positive regulation of PPARγ-target genes by DOK1.

3.6. DOK1 inhibits transcription from the c-FOS promoter

We next asked whether the effects of DOK1 on transcription are independent from or coexisting with inhibition of the RAS-ERK1/2 pathway. RAS-pulldown assays were performed in TCLs from cycling cells (Fig. 5A) or upon transfection of FL p62 DOK1 (Fig. 5B). Higher pan-RAS activity was seen in *KRASG12V* mutant SW480 than in *KRASG13D* mutant HCT116 cells. *KRAS*-WT cells (HEK293T, Caco2, HT29) were negative. Consistent with others (Songyang et al., 2001), DOK1 did not inhibit the activity of mutant RAS. Western blot analyses corroborated that DOK1 was also unable to reduce phosphorylation of ERK1/2 in starved cells that had been restimulated with EGF (10 ng/ml) for 0–30 min (Fig. 5C). As a genomic readout for DOK1-mediated inhibition of the RAS-ERK1/2 cascade (Yoshida et al., 2000), we measured transcriptional activation of the serum-response element (SRE) in the human *c-FOS* promoter (Buchwalter et al., 2004) (Fig. 5D). HCT116 cells were cotransfected with DOK1 and SRE reporter plasmids for 24 h, followed by serum deprivation for 16 h and stimulation with EGF (10 ng/ml) for additional 24 h.

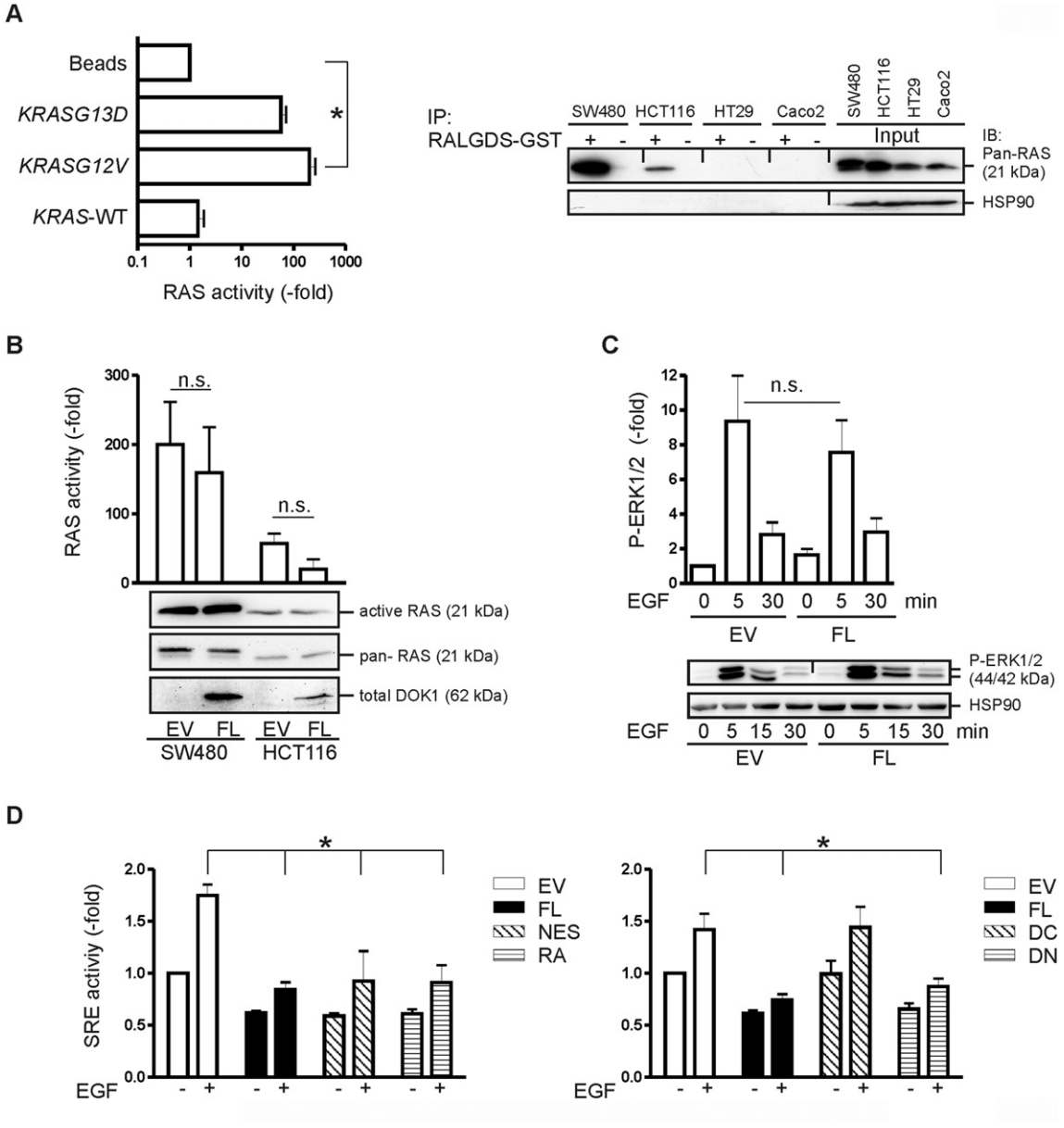

Fig. 5. DOK1 inhibits *c-FOS* promoter transcription. (A) Western blots of pulldown assays detecting active GTP-bound pan-RAS proteins in TCLs compared to total pan-RAS (input) using RALGDS-GST as a bait. Results are -fold ± S.E. ($n = 3$ per cell line, $^*p < 0.05$ *vs.* beads, Kruskal Wallis test). (B) DOK1 does not inhibit mutant RAS. Cells were transfected with EV or FL p62 DOK1 for 48 h before pulldown. Data are presented as in A ($n = 3$, n.s., two-way ANOVA). (C) DOK1 does not inhibit ERK1/2 phosphorylation. HEK293T, SW480 and HCT116 were transfected with DOK1 plasmids for 24 h, serum deprived for 16 h and restimulated with EGF (10 ng/ml) for the times indicated. Data from Western blots of TCLs are shown as in A ($n = 3$ per cell line, n.s., two-way ANOVA). (D) DOK1 inhibits the human *c-FOS* promoter. HCT116 cells were cotransfected with DOK1 and SRE reporter plasmids for 24 h followed by incubation with EGF (10 ng/ml) in serum-free medium for additional 24 h. Luciferase activity in TCLs normalized to protein content was calculated as -fold ± S.E. ($n = 3$, $^*p < 0.05$ *vs.* EV, two-way ANOVA).

Luciferase activity was decreased by FL p62 DOK1 in the basal state by 62% and upon EGF-stimulation by 49% compared with EV controls. Likewise, NES exerted an inhibition by 59% (53%) and RA by 61% (52%). Thus, FL p62 DOK1 is an inhibitor of nuclear SRE-driven transcription but not of upstream RAS-ERK1/2 signaling. DC was inert compared with a robust inhibition of DN by 34% (38%).

Thus, deletion of the PH domain but not point mutations in the PTB or NES reduced the ability of DOK1 to inhibit the SRE. Similar results were obtained from HEK293T cells, whereas SW480 cells were again unresponsive (not shown). Hence, the N-terminal part of DOK1 was sufficient for inhibition of the *c-FOS* promoter, the C-terminal part necessary for activation of PPARγ (Table S2).

3.7. DOK1 sensitizes cells to PPARγ-ligand-driven growth inhibition

To test if regulation of transcription by DOK1 translates into a decrease of cell growth, HEK293T cells were transfected with DOK1 plasmids and cultivated for 3 days followed by MTT proliferation assay. Consistently (Ling et al., 2005; Zhao et al., 2006), DOK1 did not change the basal proliferation rate compared with EV controls (data not shown). Instead, FL p62 DOK1 enhanced growth inhibition exerted by PPARγ-ligand (3 μM rosi for 3 days) to 80 ± 7% *vs.* EV (Fig. 6A). NES but not RA was as efficient as FL p62 DOK1 to augment the growth inhibitory response to rosi (82 ± 5%). DC also slowed cell growth (84 ± 2%), DN did not. Similar results were obtained from HCT116 cells, whereas SW480 cells were resistant (not shown). Thus, the C-terminal part of DOK1 with a functional PTB domain is necessary for PPARγ activation and growth inhibition.

In contrast, DOK1-siRNA reduced the sensitivity of human GC (Burgermeister et al., 2011) and CRC cells to PPARγ-ligand-mediated growth inhibition. Proliferation was enhanced (by 23% SW480; 42% AGS) compared to control-siRNA (Fig. 6B). Similar results were collected from HCT116, HT29 and MKN45 cells (not shown).

To distinguish ligand- from receptor-mediated effects, HEK293T cells were transfected with GFP-PPARγ plasmids, and cell growth was determined after 3 days in absence of ligand (Fig. 6C). Cells which received S84A or Dbox mutants grew faster than those with WT-PPARγ (131% and 116% *vs.* WT). The H7 mutant, with a deletion of helix 7 in the LBD that renders PPARγ insensitive to ligands, increased growth to 124% *vs.* WT. Thus, the proposed DOK1 interaction sites on PPARγ (S84 and Dbox) support the intrinsic anti-proliferative activity of PPARγ even in absence of exogenous ligand.

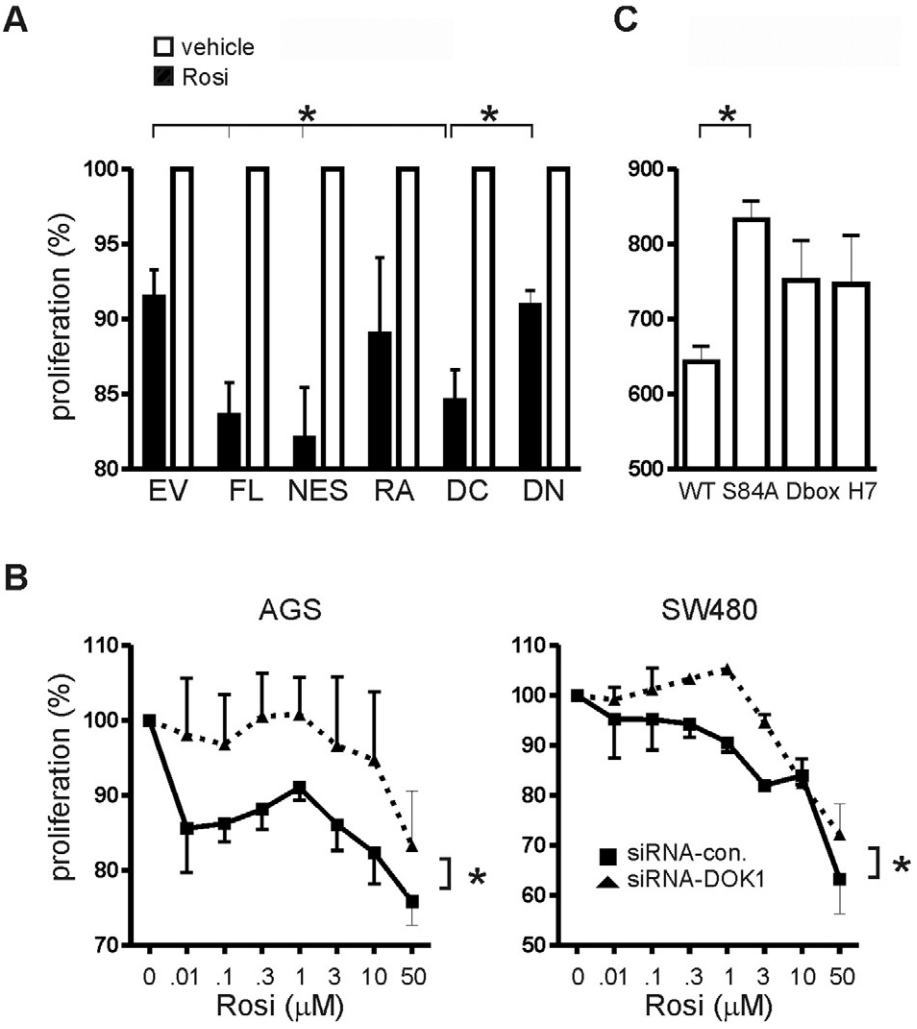

Fig. 6. DOK1 augments PPARγ-ligand-mediated inhibition of cell proliferation. (A) PTB and C-terminal domains, but not the N-terminal part of DOK1, are required for growth inhibition. HCT116 were transfected with DOK1 plasmids, and proliferation was measured after 5 days in presence of rosi (3 μM). O.D. values from MTT assays were calculated as % ± S.E. ($n = 3$, *p < 0.05 DOK1 + rosi *vs.* EV + rosi; two-way ANOVA). (B) DOK1 knock-down enhances cell growth. Cells were transfected with siRNA, and proliferation was determined as in A ($n = 3$, *p < 0.05 DOK1- *vs.* control-siRNA, two-way ANOVA). (C) Growth inhibition is PPARγ-receptor dependent. HEK293T cells were transfected with PPARγ plasmids for 72 h in absence of ligand. Data are shown as in A ($n = 3$, *p < 0.05 *vs.* WT, one-way ANOVA).

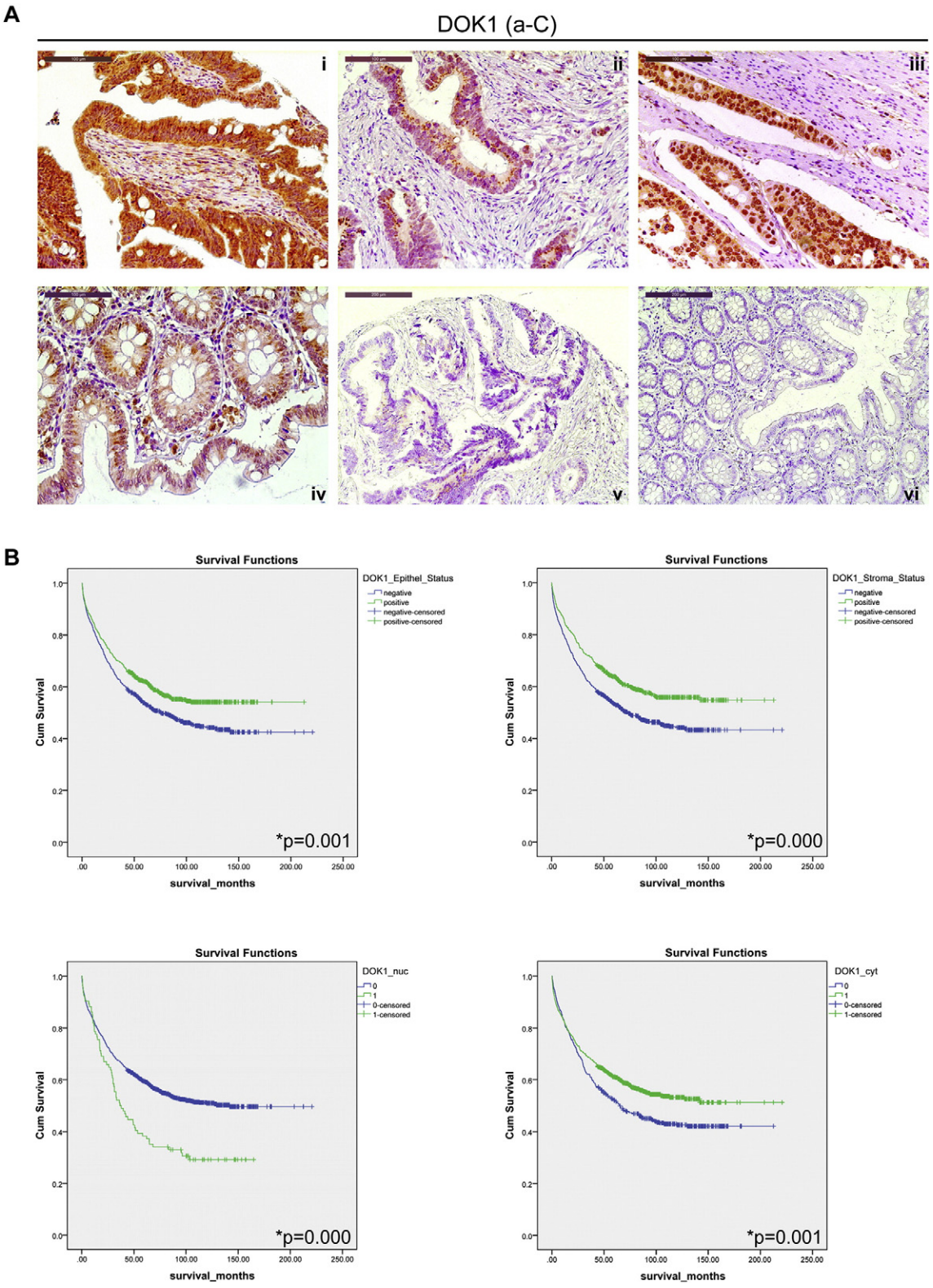

Fig. 7. Compartmentalization of DOK1 predicts prognosis of CRC patients. (A) Immunohistochemistry (IHC) with DOK1 anti-C Ab (ab8112) on tissue microarrays (TMAs) with tumor (TU, $n = 1648$) specimens from CRC patients. Representative images are shown. DOK1 (brown color) was localized to the tumor cells in the cytoplasm (*i*), the apical perinuclear area (*ii*) or the nucleus (*iii*). Note the mixed pattern of DOK1 staining (positive control) in the normal colon glands both in epithelial (enterocytes) and stromal cells of the lamina propria (*iv*). DOK1 positivity was lost in a subset of tumors (*v*) and was absent in the secondary Ab only (negative control) staining (*vi*). Magnifications 200×. (B) Loss of DOK1 protein expression predicts poor survival in CRC patients. Kaplan–Meier curves of patient overall survival (OS). Upper panels: OS for DOK1 tumor and stroma expression; Lower panels: OS for nuclear and cytoplasmic DOK1 expression in the tumor. Nuclear localization of DOK1 correlates with poor, cytoplasmic DOK1 with improved prognosis. Data are surviving proportions *vs.* months ($n = 1492$,*$p < 0.05$ log-rank tests). Values for tumor-specific survival (TSS) and median survival are presented in Table S4.

3.8. Subcellular compartmentalization of DOK1 protein predicts survival of CRC patients

To finally assess the clinical relevance of DOK1 protein expression *in situ*, we stained tissue microarrays (TMAs) by immunohistochemistry (IHC) comprising a large cohort of CRC patients ($n = 1648$). Anti-C Ab (ab8112) (Siouda et al., 2014) was used because it detected the most abundant DOK1 variants (FL p62 and p44) in human tissues. DOK1 protein was present in the nucleus and cytoplasm of epithelial and stromal cells in the normal colon mucosa (*e.g.* enterocytes and leukocytes) and in tumor cells. Apical perinuclear accumulation of DOK1 protein was also observed (Fig. 7A).

Frequency and intensity of DOK1 staining were correlated to clinicopathological factors. The overall DOK1 positivity score in tumor cells was reduced (*p < 0.05; Fisher exact tests) with increasing tumor stage (UICC) and the pTNM-categories local tumor growth (T), nodal spread (N) and tumor grade (G); in stroma cells with T-, N- and M-categories and UICC stage (**S3**, Table S3). There was no association with age, gender or anatomical localization of the tumor. Loss of DOK1 in tumor cells ($n = 1492$ cases) predicted poor overall (OS) and tumor-specific (TSS) survival (5 and 10-year OS [TSS]: DOK1 negative 53.7 and 44.3 [63.8 and 59.2] *vs.* 62.0 and 54.1 [70.8 and 67.4] DOK1 positive; $^*p = 0.001$ [0.003] log-rank test). Importantly, expression of cytoplasmic DOK1 correlated with improved prognosis (52.1 and 42.5 [62.2 and 57.3] *vs.* 61.1 and 53.3 [70.0 and 66.7]; $^*p = 0.001$ [0.005]). In contrast, nuclear localization of DOK1 predicted poor outcome (59.4 and 50.9 [68.4 and 64.3] *vs.* 38.3 and 29.1 [51.1 and 49.6]; $^*p = 0.000$ [0.011]). Similar results were obtained for tumor and stroma (Fig. 7B, Table S4).

Separate analysis of survival for patient subgroups according to their metastatic status (**S4**, Table S5) revealed that DOK1 expression was prognostic in M0 but not in M1 cases. M1 was defined by metastasis to distant organs beyond regional lymph nodes. Similar results were obtained for UICC stages (**S5**, Table S6), indicative of a prognostic relevance for DOK1 in early stages of non-metastatic CRC. Cox regression was carried out on all parameters with $p < 0.1$ in univariate survival analysis (Metzger et al., 2016). Seven independent prognostic parameters remained in the model after applying backward logistic regression, including: gender, age, nodal spread (N), invasion to lymphatic vessels (L), invasion to veins (V), tumor stage (UICC) and cytoplasmic DOK1 expression [hazard ratio (HR) = 0.809 (0.687–0.953); $^*p = 0.011$] (Table S7). Clinical correlates were confirmed in a smaller cohort of CRC patients ($n = 40$) and normal colon ($n = 8$) tissue specimens with anti-N Ab (A3) which detected the predominant DOK1 variant (p37) in transformed human cell lines (**S6**, Table S8).

In sum, loss of DOK1 protein expression was a frequent event in CRC and conferred poor clinical outcome. Importantly, patients with gain of nuclear DOK1 suffered from a worse prognosis.

3.9. Genomic alterations of DOK1 are rare events in CRC

To elucidate whether the observed changes in DOK1 protein are associated with *DOK1* gene alterations, *in silico* mining of CRC patients' data was done using the cBioportal of Cancer Genomics (Cerami et al., 2012; Gao et al., 2013). *DOK1* gene alterations were found in 3% of the cases ($n = 628$; TCGA_Provisional (Network, 2012)) and in 4% of human cancer cell lines ($n = 1019$; CCLE), mainly due to changes in transcript levels, and the somatic mutation rate was low (< 0.3%). Overall alteration rates were < 10% in 86 cancer studies from > 15 tumor entities. To see if *DOK1* gene alterations correlate with patient survival, information was retrieved for a 9-gene signature covering the RAS-signaling pathway (*EGFR*, *KRAS*, *NRAS*, *BRAF*, *MEK1*, *ERK2*, *CAV1*, *PPARG*, *DOK1*) (**S7**). Within this cooperative network, the latter 3 genes were RAS-pathway inhibitors ("tumor suppressors") (Ogino et al., 2009; Burgermeister et al., 2011), the first 6 genes oncogenic drivers (Misale et al., 2012; Network, 2012). Median month overall (57.19 *vs.* 99.93; log-rank test $p = 0.176$; $n = 545$) and disease-free (63.37 *vs.* > 140; log-rank test $^*p = 0.044$; $n = 531$) survival was lower in CRC patients with than without alterations in the query genes. In contrast to *CAV1* ($^*p = 0.00714$), the contribution of *DOK1* gene alterations to survival was not significant.

RT-qPCR analyses (**S8**) on frozen CRC tissue samples ($n = 10$) from matched normal colon (NC), primary tumor (TU) and liver metastases (M) (stage IV) failed to revealed differences in *DOK1* mRNA expression, neither between cases with good prognosis (no post-operative disease recurrence, $n = 13$) *vs.* disease relapse (distant metastasis, $n = 13$) nor in stage II ($n = 26$) and IV ($n = 10$) tumors regarding *KRAS* and *BRAF* mutations. In contrast to down-regulation of *PPARG* (Ogino et al., 2009) and *CAV1* mRNAs, *DOK1* mRNA was maintained in tumors and metastases, proposing a functional role for DOK1 in CRC progression.

RT-qPCRs using primer pairs against the N- and the C-terminal part (Burgermeister et al., 2011) of the FL *DOK1* cDNA in human cell lines (**S8**) evinced that the complete mRNA was present. CRC cell lines had even higher levels of *DOK1* mRNA than NC tissue, suggesting a residual function for DOK1 in malignant cells. *Dok1* mRNA was also detected in primary enterocytes isolated from the intestines of C57BL6J mice (**S8**), confirming results in murine CRC (Friedrich et al., 2013).

Thus, subcellular patterns of DOK1 protein expression but not changes in *DOK1* mRNA were associated with clinical factors in human CRC. Conclusively, we could show that subcellular compartmentalization of DOK1 contributes to progression of CRC and predicts patients' survival (see model at a glance in Fig. 8). Specifically, cytoplasmic DOK1 protein expression was an independent positive prognostic factor for non-metastatic CRC.

4. Discussion

In the present study, we describe a role for compartmentalization of DOK1 as a predictor of patient's survival in CRC. We characterized DOK1 as a regulator of transcription in contrast to signaling inhibition at the plasma membrane. Consistent with reports from leukemias (Lee et al., 2004, 2007), we had previously identified a p37–44 DOK1 variant in human GC cells corresponding to the N-terminal part of FL p62 DOK1 (Burgermeister et al., 2011). We now demonstrate that human CRC cells retain truncated DOK1 variants as well, pointing at a more general principle. This held also true for transformed tissues from human and mice *in vivo*, consistent with a frequent loss of DOK1 in other cancer types (Berger et al., 2010; Balassiano et al., 2011; Saulnier et al., 2012).

The hitherto unknown functions of small DOK1 variants in cancer cells were explored using expression plasmids for p44 DC (Kobayashi et al., 2009) and p33 DN (Lee et al., 2004, 2007) which covered the C- and N-terminal domains of FL p62 DOK1 (Songyang et al., 2001) (see model in Fig. 1C). Endogenous p37 and p33 DN were located in the nucleus, while FL p62 DOK1 and p44 DC were confined to the perinuclear area of the cytoplasm and at membranes colocalizing with the endoplasmic reticulum (ER). (Lee et al., 2004, 2007) presented leukemia patients with C-terminally truncated DOK1^{BCCL13} (p33–35) mutants in the nucleus due to a frame shift that introduced a NLS and a premature stop codon. Thus, cancer cells seem to retain nuclear (C-terminally truncated) (Lee et al., 2004, 2007) and cytoplasmic (N-terminally truncated) (Kobayashi et al., 2009) DOK1 isoforms.

Those may be potentially defective variants that remain upon transformation and loss of FL p62 DOK1 as a functional tumor suppressor (Berger et al., 2010; Balassiano et al., 2011; Saulnier et al., 2012).

Our functional studies assigned the regions for PPARγ activation and growth inhibition to the C-terminal part of DOK1, whereas the N-terminal part of DOK1 was required for inhibition of the *c-FOS* promoter. The DN and DC truncation variants were both sufficient for interaction with PPARγ provided they had a functional PTB domain. Notably, mutation of the PTB arginine residues (R207–223) (Zhang et al., 2004; Uhlik et al., 2005; Oxley et al., 2008) in DOK1 and the MAPK-phosphorylation site (S84) in PPARγ1 abolished the interaction. The 83A**S**PPYYSEKT92 site

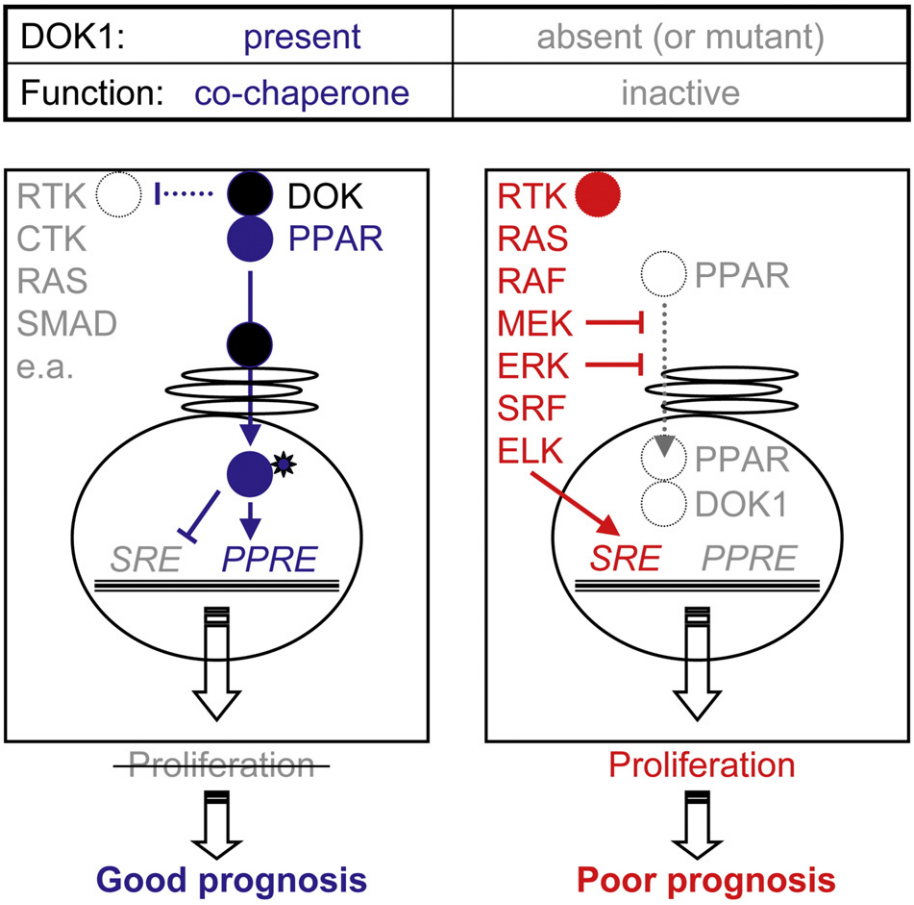

Fig. 8. Signaling model at a glance. In cells with FL p62 DOK1 at the membrane or cytoplasmic p44 DC mutant, oncogenic signaling of many target proteins is inhibited (such as RTK, CTK, SMAD, RAS, ELK1 e.a.) leading to reduction of *SRE* transcription (which drives cells into G1-S phase) and activation of *PPRE* transcription (which dampens cell proliferation), two exemplary read-outs used in the present study. PPARγ-agonist (star) further augments PPARγ-mediated growth inhibition, resulting in a good prognosis for patients' survival. Mechanistically, DOK1 may act as a "co-chaperone" for ligand-dependent nuclear translocation of PPARγ across the ER and nuclear pores. In tumor cells with loss of FL p62 DOK1 or accumulation of nuclear p33 DN mutant, oncogenic signaling (depicted here exemplary for the RAS-ERK1/2-ELK1-SRF pathway) is unimpeded leading to enhanced *SRE* and reduced *PPRE* transcription, resulting in tumor cell proliferation and a poor prognosis. Mechanistically, MEK1 and ERK1/2 inhibit nuclear translocation of PPARγ by promoting its export to the cytoplasm and inactivation by phosphorylation. Legend: red = active oncogene; blue black = active tumor suppressor; grey = inactive protein.

is phosphorylated by ERK1/2 (Diradourian et al., 2005), next to other serines by CDK5 (Choi et al., 2010) or CKII (von Knethen et al., 2010) and resembles the NPX**Y** (Uhlik et al., 2005) motif bound by PTB domains also in an unphosphorylated state. Mutation of the leucine-rich NES in DOK1 348LLKAKLTDP **KEDPIYDEPEG**367 (Niu et al., 2006), which interacts with the zinc-finger **"hakai** tyrosine-binding domain" (HYB) of the E3 ligase hakai (Mukherjee et al., 2012) and is phosphorylated by SRC (Songyang et al., 2001), together with deletion of the Dbox motif 149DLNCRIHKKSRN160 (Zechel et al., 1994) in the second zinc-finger of the PPARγ1 DBD also prevented complex formation (**S2**). Both PPARγ mutations accelerated cell growth, confirming their defect to interact and cooperate with DOK1.

FL p62 DOK1 and DC activated PPARγ without being translocated to the nucleus, whereas DN acted as a "nuclear trapping" mutant for PPARγ. This pattern (Table S2) was consistent with the presence or absence of N-terminal NLS and C-terminal NES motifs in the DOK1 mutants: FL (**NLS**$^+$, **NES**$^+$) and DC (**NLS**$^-$, **NES**$^+$) were exported to the cytoplasm *via* their NES. DN (**NLS**$^+$, **NES**$^-$) was confined to the nucleus *via* a predicted NLS, as described for DOK7 (Hamuro et al., 2008). Thus, DOK1 may act as a "co-chaperone" that brings PPARγ into proximity of the nuclear envelope which is continuous with the ER. PPARs as members of the nuclear receptor superfamily harbour at least one NLS in the DBD (Kumar et al., 2006; Iwamoto et al., 2011) and are transported across the nuclear pores by the default RAN GTPase-importin system. DOK1 may thus rather facilitate the release of PPARγ from cytosolic sequestors (as shown for CAV1 or MEK1) (von Knethen et al., 2010; Burgermeister et al., 2011) (**S9**) than acting as a specific nuclear import shuttle for PPARγ. Mechanistically, DOK1 (alike MEK1) may also contribute to recycling of PPARγ back to the cytosol for reloading with ligand.

Nonetheless, DOK1 interacts with other transcription factors such as SMAD3 and 4 (Yamakawa et al., 2002), and impacts on multiple signaling pathways including JAK-STAT and NFκB relevant for proliferation, apoptosis and inflammation (Downer et al., 2013; Nold-Petry et al., 2015). Our data confirmed (Yoshida et al., 2000) that DOK1 inhibits the *c-FOS* promoter, a mechanism which involves serum response factor (SRF) and ternary complex factors (like ELK1) as shown for DOK4 (Baldwin et al., 2007). Thus, the causal link between DOK1 and RAS-signaling in CRC remains unproven and is expected to involve higher complexity than studied here exemplarily for PPARγ.

Taken together, our data propose that inhibition of signaling by DOK1 is separated from its effect on transcription by the following mechanisms: (i) across cell compartments and (ii) *via* different protein variants (domains). Thereby, DOK1 may switch from membrane-bound towards soluble cytosolic-nuclear targets. This alternative route shall come into place in cases where failure to inhibit plasma membrane-bound targets is common, *e.g.* due to constitutive RTK-RAS-signaling upon mutation or amplification events in cancers. This flexibility of DOK1 effector profiles may be part of a cellular defense response to exploit the remaining "downstream" tumor suppressive potential of DOK1

in presence of "upstream" over-feeding of signal input. The DOK protein family forms homo- and heterodimers (Mashima et al., 2009). Residual small DOK1 variants in cancer cells may hijack this escape mechanism to interfere with tumor growth even upon loss of FL p62 DOK1.

In the context of translational relevance of our study, we showed that overexpression of DOK1 reduced, whereas knock-down of DOK1 enhanced cell proliferation, consistent with a decrease of DOK1 protein expression along tumor progression in CRC patients. Genomic alterations in a 9-gene signature covering the RAS-pathway correlated with poor survival in CRC patients. There was no association of *DOK1* mRNA with disease recurrence or *KRAS-BRAF* mutations, suggesting that DOK1 still plays a role in established tumors. In line with this hypothesis, we demonstrated that subcellular compartmentalization of DOK1 protein is predictive for CRC patient's survival. These findings may have implications for therapy. Expression of DOK1 mRNA and protein can be up-regulated by PPARγ-agonists (Hosooka et al., 2008; Burgermeister et al., 2011) (**S10**), and pharmacological induction of *Pparγ-Dok1-Cav1* genes made RAS drugable in a preclinical model of murine CRC (Friedrich et al., 2013). CRC patients with *RAS* mutations and a subset of *RAS*-WT tumors do not respond to clinical therapies against the EGF receptor (Misale et al., 2012). Since DOK1 addresses alternative targets (*e.g.* transcription factors) downstream of multiple signaling pathways (including RAS), it may be suitable for future treatment strategies in human cancers.

5. Conclusions

Our study demonstrated that forward translation of a cell-based signaling model predicted subcellular compartmentalization of DOK1 in patients. Cytoplasmic expression of DOK1 (conferred by C-terminal domains) correlated with improved prognosis in non-metastatic CRC and evoked growth inhibition in human cancer cells, whereas nuclear DOK1 (conferred by N-terminal domains) predicted poor survival and was inactive in cells. The subcellular localization of DOK1 may therefore serve as a possible future prognostic marker for CRC progression. DOK1–PPARγ interaction and expression was increased by PPARγ-agonist. Hence, RTK-RAS signaling may be indirectly drugable "from within the cell" by the insulin sensitizer rosiglitazone (Avandia®), constituting a potential future target for cancer therapy.

Disclosure of potential conflicts of interest

The authors have nothing to declare.

Funding

Deutsche Krebshilfe (#108287, #111086), German Cancer Research Center (DKFZ-MOST) (Ca158), Deutsche Forschungsgemeinschaft (DFG) (BU2285, SFB 824 TP B1) and ZOBEL (Center of Geriatric Biology and Oncology) and Land Baden-Württemberg (Perspektivförderung). The funders had no role in study design, data collection, data analysis, interpretation and writing of the report.

Author contributions

All authors cooperated and contributed to, critically reviewed and approved the manuscript. EB and ME defined the research theme. TF, MS, TG and KPJ designed methods and carried out the experiments. TF, MS, TG and EB analysed the data and interpreted the results. EB wrote the paper. CR, HMB and TG analysed and interpreted immunostainings. CR and KPJ provided samples and reviewed the manuscript.

Acknowledgements

We want to thank Frank Herweck, Sandra Krueger and Sandra Schneider for excellent technical assistance. We are very grateful to Prof. Rony Seger (Weizmann Institute of Science, Rehovot, Israel) for reviewing the manuscript, discussion and advice.

Appendix A. Supplementary data

Supplementary data to this article can be found online at http://dx.doi.org/10.1016/j.ebiom.2016.05.003.

References

Adams, M., Reginato, M.J., et al., 1997. Transcriptional activation by peroxisome proliferator-activated receptor gamma is inhibited by phosphorylation at a consensus mitogen-activated protein kinase site. J. Biol. Chem. 272 (8), 5128–5132.
Balassiano, K., Lima, S., et al., 2011. Aberrant DNA methylation of cancer-associated genes in gastric cancer in the European Prospective Investigation into Cancer and Nutrition (EPIC-EURGAST). Cancer Lett. 311 (1), 85–95.
Baldwin, C., Bedirian, A., et al., 2007. Identification of Dok-4b, a Dok-4 splice variant with enhanced inhibitory properties. Biochem. Biophys. Res. Commun. 354 (3), 783–788.
Banks, A.S., McAllister, F.E., et al., 2015. An ERK/Cdk5 axis controls the diabetogenic actions of PPARgamma. Nature 517 (7534), 391–395.
Berger, A.H., Niki, M., et al., 2010. Identification of DOK genes as lung tumor suppressors. Nat. Genet. 42 (3), 216–223.
Boger, C., Warneke, V.S., et al., 2015. Integrins alphavbeta3 and alphavbeta5 as prognostic, diagnostic, and therapeutic targets in gastric cancer. Gastric Cancer 18 (4), 784–795.
Buchwalter, G., Gross, C., et al., 2004. Ets ternary complex transcription factors. Gene 324, 1–14.
Burgermeister, E., Chuderland, D., et al., 2007. Interaction with MEK causes nuclear export and downregulation of peroxisome proliferator-activated receptor gamma. Mol. Cell. Biol. 27 (3), 803–817.
Burgermeister, E., Friedrich, T., et al., 2011. The Ras inhibitors caveolin-1 and docking protein 1 activate peroxisome proliferator-activated receptor gamma through spatial relocalization at helix 7 of its ligand-binding domain. Mol. Cell. Biol. 31 (16), 3497–3510.
Cerami, E., Gao, J., et al., 2012. The cBio cancer genomics portal: an open platform for exploring multidimensional cancer genomics data. Cancer Discov. 2 (5), 401–404.
Choi, J.H., Banks, A.S., et al., 2010. Anti-diabetic drugs inhibit obesity-linked phosphorylation of PPARgamma by Cdk5. Nature 466 (7305), 451–456.
Demers, A., Caron, V., et al., 2009. A concerted kinase interplay identifies PPARgamma as a molecular target of ghrelin signaling in macrophages. PLoS One 4 (11), e7728.
Diradourian, C., Girard, J., et al., 2005. Phosphorylation of PPARs: from molecular characterization to physiological relevance. Biochimie 87 (1), 33–38.
Downer, E.J., Johnston, D.G., et al., 2013. Differential role of Dok1 and Dok2 in TLR2-induced inflammatory signaling in glia. Mol. Cell. Neurosci. 56, 148–158.
Ebert, M.P., Tanzer, M., et al., 2012. TFAP2E-DKK4 and chemoresistance in colorectal cancer. N. Engl. J. Med. 366 (1), 44–53.
Friedrich, T., Richter, B., et al., 2013. Deficiency of caveolin-1 in Apcmin/+ mice promotes colorectal tumorigenesis. Carcinogenesis 34 (9), 2109–2118.
Gao, J., Aksoy, B.A., et al., 2013. Integrative analysis of complex cancer genomics and clinical profiles using the cBioPortal. Sci. Signal. 6 (269), l1.
Good, M.C., Zalatan, J.G., et al., 2011. Scaffold proteins: hubs for controlling the flow of cellular information. Science 332 (6030), 680–686.
Hamuro, J., Higuchi, O., et al., 2008. Mutations causing DOK7 congenital myasthenia ablate functional motifs in Dok-7. J. Biol. Chem. 283 (9), 5518–5524.
Hosooka, T., Noguchi, T., et al., 2001. Inhibition of the motility and growth of B16F10 mouse melanoma cells by dominant negative mutants of Dok-1. Mol. Cell. Biol. 21 (16), 5437–5446.
Hosooka, T., Noguchi, T., et al., 2008. Dok1 mediates high-fat diet-induced adipocyte hypertrophy and obesity through modulation of PPAR-gamma phosphorylation. Nat. Med. 14 (2), 188–193.
Hubert, P., Ferreira, V., et al., 2000. Molecular cloning of a truncated p62Dok1 isoform, p22Dok(del). Eur. J. Immunogenet. 27 (3), 145–148.
Ingold Heppner, B., Behrens, H.M., et al., 2014. HER2/neu testing in primary colorectal carcinoma. Br. J. Cancer 111 (10), 1977–1984.
Iwamoto, F., Umemoto, T., et al., 2011. Nuclear transport of peroxisome-proliferator activated receptor &alpha. J. Biochem. 149 (3), 311–319.
Janas, J.A., Van Aelst, L., 2011. Oncogenic tyrosine kinases target Dok-1 for ubiquitin-mediated proteasomal degradation to promote cell transformation. Mol. Cell. Biol. 31 (13), 2552–2565.
Jhawer, M., Goel, S., et al., 2008. PIK3CA mutation/PTEN expression status predicts response of colon cancer cells to the epidermal growth factor receptor inhibitor cetuximab. Cancer Res. 68 (6), 1953–1961.
Jiang, X., Huang, L., et al., 2015. Photoactivation of Dok1/ERK/PPARgamma signaling axis inhibits excessive lipolysis in insulin-resistant adipocytes. Cell. Signal. 27 (7), 1265–1275.
Kobayashi, R., Patenia, R., et al., 2009. Targeted mass spectrometric analysis of N-terminally truncated isoforms generated via alternative translation initiation. FEBS Lett. 583 (14), 2441–2445.

Kodach, L.L., Wiercinska, E., et al., 2008. The bone morphogenetic protein pathway is inactivated in the majority of sporadic colorectal cancers. Gastroenterology 134 (5), 1332–1341.
Kononen, J., Bubendorf, L., et al., 1998. Tissue microarrays for high-throughput molecular profiling of tumor specimens. Nat. Med. 4 (7), 844–847.
Kumar, S., Saradhi, M., et al., 2006. Intracellular localization and nucleocytoplasmic trafficking of steroid receptors: an overview. Mol. Cell. Endocrinol. 246 (1–2), 147–156.
Lee, S., Roy, F., et al., 2004. Frameshift mutation in the Dok1 gene in chronic lymphocytic leukemia. Oncogene 23 (13), 2287–2297.
Lee, S., Huang, H., et al., 2007. Dok1 expression and mutation in Burkitt's lymphoma cell lines. Cancer Lett. 245 (1–2), 44–50.
Ling, Y., Maile, L.A., et al., 2005. DOK1 mediates SHP-2 binding to the alphaVbeta3 integrin and thereby regulates insulin-like growth factor I signaling in cultured vascular smooth muscle cells. J. Biol. Chem. 280 (5), 3151–3158.
Mashima, R., Hishida, Y., et al., 2009. The roles of Dok family adapters in immunoreceptor signaling. Immunol. Rev. 232 (1), 273–285.
Mashima, R., Honda, K., et al., 2010. Mice lacking Dok-1, Dok-2, and Dok-3 succumb to aggressive histiocytic sarcoma. Lab. Investig. 90 (9), 1357–1364.
Metzger, M.L., Behrens, H.M., et al., 2016. MET in gastric cancer — discarding a 10% cutoff rule. Histopathology 68 (2), 241–253.
Miah, S., Goel, R.K., et al., 2014. BRK targets Dok1 for ubiquitin-mediated proteasomal degradation to promote cell proliferation and migration. PLoS One 9 (2), e87684.
Misale, S., Yaeger, R., et al., 2012. Emergence of KRAS mutations and acquired resistance to anti-EGFR therapy in colorectal cancer. Nature 486 (7404), 532–536.
Mukherjee, M., Chow, S.Y., et al., 2012. Structure of a novel phosphotyrosine-binding domain in Hakai that targets E-cadherin. EMBO J. 31 (5), 1308–1319.
Network, T.C.G.A., 2012. Comprehensive molecular characterization of human colon and rectal cancer. Nature 487 (7407), 330–337.
Niu, Y., Roy, F., et al., 2006. A nuclear export signal and phosphorylation regulate Dok1 subcellular localization and functions. Mol. Cell. Biol. 26 (11), 4288–4301.
Nold-Petry, C.A., Lo, C.Y., et al., 2015. IL-37 requires the receptors IL-18Ralpha and IL-1R8 (SIGIRR) to carry out its multifaceted anti-inflammatory program upon innate signal transduction. Nat. Immunol. 16 (4), 354–365.
Ogino, S., Shima, K., et al., 2009. Colorectal cancer expression of peroxisome proliferator-activated receptor gamma (PPARG, PPARgamma) is associated with good prognosis. Gastroenterology 136 (4), 1242–1250.
Oxley, C.L., Anthis, N.J., et al., 2008. An integrin phosphorylation switch: the effect of beta3 integrin tail phosphorylation on Dok1 and talin binding. J. Biol. Chem. 283 (9), 5420–5426.
Saulnier, A., Vaissiere, T., et al., 2012. Inactivation of the putative suppressor gene DOK1 by promoter hypermethylation in primary human cancers. Int. J. Cancer 130 (11), 2484–2494.
Shinohara, H., Yasuda, T., et al., 2004. Dok-1 tyrosine residues at 336 and 340 are essential for the negative regulation of Ras-Erk signalling, but dispensable for rasGAP-binding. Genes Cells 9 (6), 601–607.
Shinohara, H., Inoue, A., et al., 2005. Dok-1 and Dok-2 are negative regulators of lipopolysaccharide-induced signaling. J. Exp. Med. 201 (3), 333–339.
Siouda, M., Yue, J., et al., 2012. Transcriptional regulation of the human tumor suppressor DOK1 by E2F1. Mol. Cell. Biol.
Siouda, M., Frecha, C., et al., 2014. Epstein–Barr virus down-regulates tumor suppressor DOK1 expression. PLoS Pathog. 10 (5), e1004125.
Songyang, Z., Yamanashi, Y., et al., 2001. Domain-dependent function of the rasGAP-binding protein p62Dok in cell signaling. J. Biol. Chem. 276 (4), 2459–2465.
Uhlik, M.T., Temple, B., et al., 2005. Structural and evolutionary division of phosphotyrosine binding (PTB) domains. J. Mol. Biol. 345 (1), 1–20.
van Dijk, T.B., van Den Akker, E., et al., 2000. Stem cell factor induces phosphatidylinositol 3′-kinase-dependent Lyn/Tec/Dok-1 complex formation in hematopoietic cells. Blood 96 (10), 3406–3413.
von Knethen, A., Tzieply, N., et al., 2010. Casein-kinase-II-dependent phosphorylation of PPARgamma provokes CRM1-mediated shuttling of PPARgamma from the nucleus to the cytosol. J. Cell Sci. 123 (Pt 2), 192–201.
Yamakawa, N., Tsuchida, K., et al., 2002. The rasGAP-binding protein, Dok-1, mediates activin signaling via serine/threonine kinase receptors. EMBO J. 21 (7), 1684–1694.
Yasuda, T., Shirakata, M., et al., 2004. Role of Dok-1 and Dok-2 in myeloid homeostasis and suppression of leukemia. J. Exp. Med. 200 (12), 1681–1687.
Yoshida, K., Yamashita, Y., et al., 2000. Mediation by the protein-tyrosine kinase Tec of signaling between the B cell antigen receptor and Dok-1. J. Biol. Chem. 275 (32), 24945–24952.
Zechel, C., Shen, X.Q., et al., 1994. The dimerization interfaces formed between the DNA binding domains of RXR, RAR and TR determine the binding specificity and polarity of the full-length receptors to direct repeats. EMBO J. 13 (6), 1425–1433.
Zhang, Y., Yan, Z., et al., 2004. Molecular basis of distinct interactions between Dok1 PTB domain and tyrosine-phosphorylated EGF receptor. J. Mol. Biol. 343 (4), 1147–1155.
Zhao, M., Janas, J.A., et al., 2006. Dok-1 independently attenuates Ras/mitogen-activated protein kinase and Src/c-myc pathways to inhibit platelet-derived growth factor-induced mitogenesis. Mol. Cell. Biol. 26 (7), 2479–2489.